ISME

Effect of Volute and Rotor Widths on Squirrel Cage Fan Performance and Velocity Profiles

A.H. Dehkordi[*]
Professor

N. Montazerin[†]
Professor

E. Damangir[‡]
Assistant Professor

S.M. Rezaei Niya[§]
MSc. Graduate

The volute of a squirrel cage fan controls the flow field through the rotor and therefore the complete fan. Performance tests on fans with four rotors of the same diameter but with different widths, inside two different volutes showed that larger volute widths flatten the fan characteristics curve and allow a larger maximum volumetric flow into the fan. When the volute width is fixed, the performance curves closely overlap and the rotor width only changes the maximum flow rate. The velocity profiles after the rotor were measured using laser Doppler anemometry for four different fans. They show that in each of the four volute/rotor combinations, the flow out of the rotor is not uniform at different peripheral angles. This pattern changes with volute width and at different operating conditions. At angular positions closer to fan exit where the cross section is larger and the volute resistance is smaller, more flow exits the rotor. This flow has a shorter path inside the volute before it reaches the fan exit and therefore a higher efficiency ensues.

Keywords: Squirrel cage fan, laser Doppler anemometry, rotor width; volute, fan performance, velocity profiles

1 Introduction

Squirrel cage fans are the air driving apparatus for many heating and ventilating systems. The advantages of such fans are low cost, small noise and large flow rates [1]. Figure 1 shows the overall schematic of the fan plus its important dimensions. The available research on the squirrel cage fan follows three purposes:

1. Parametric performance studies on the fan configuration for different geometries [2]-[10];
2. Trying to understand the flow field inside the fan [11] - [19];
3. Modeling the complicated flow inside the rotor and the volute [21][22].

Here like any other centrifugal turbo machine, correct selection of rotor and volute dimensions depends on a prior knowledge of flow and loss mechanisms. A known draw back that contributes to the low efficiency of the squirrel cage fan is that the flow must turn 90° from the inlet to the rotor. It then enters the blades in the meridional plane at a mixed angle [16], figure 2. There is a separation zone behind the inlet and the bulk of the flow turns near the back plate. This separation zone occupies about one third to half of the rotor, produces

[*] Mechanical Engineering Department, Amirkabir University of Technology
[†]Corresponding Author, Mechanical Engineering Department, Amirkabir University of Technology,
E-mail: mntzrn@aut.ac.ir
[‡] Mechanical Engineering Department, Amirkabir University of Technology
[§] Mechanical Engineering Department, Amirkabir University of Technology

complicated three-dimensional re-circulating flow inside the volute and restricts the through flow. A significant portion of the kinetic energy is lost through interaction of the main flow with this virtually inactive region. Although the required static pressure distribution to turn the flow in the volute is incompatible with a uniform velocity profile, a smaller separation provides more aerodynamic flow inside the fan.

As for the volute, the data on centrifugal compressors and pumps confirms that skin friction based models of the vane-less diffuser is flawed and does not match experimental data for pressure recovery or total pressure loss [23], [24], and [25]. Therefore other loss mechanisms in a volute should be taken into account. They include: 1)Mixing between jets and wakes that come out of the rotor blades; 2) Recirculation in the stall cell behind the inlet that returns into the rotor when the fan is throttled; 3) Axially and circumferentially non uniform pressure fields; 4)Flow turning round the volute. Item 4 is a part of the subject of this study.

Volute dimensions (width, spread angle, cut-off radius and angle) have controlling effects on the flow through the rotor. The common fan design procedure is to set the rotor diameter as a base and optimize performance with variations in other rotor and then volute parameters [10]. They choose the rotor exit to inlet area ratio for restricted separation. A $4b/D_1=1.0$ corresponds to the area ratio of unity which would make a very narrow rotor. For any area ratio smaller than 1.5, fan width as compared to its outlet cross section would be very small and different to what is usual in ventilation systems. The suggested range is 1.75 to 2.0 but results are also available for the range 1.0-4.0 [1], [19], and [16], [7]. They show optimum head and efficiency for the range 1.84 and 2.6. Although a larger volute spread angle allows more flow through the rotor [10] but the ensuing larger flow coefficient makes the flow through the blades less aerodynamic [10]. For any rotor, it is possible to find an optimum volute spread angle that produces minimum loss in a limited space. This balances the advantage of a larger flow rate through the rotor with the desire for a smaller overall fan size and more aerodynamic flow through the fan. It is not known if there is a similar trend for the volute width.

There is also disagreement for the selection of relative rotor and volute widths. Some suggest a volute width as close as possible to the rotor width just to allow for inlet lip intrusion and manufacturing tolerances [10] and expect efficiency reduction if B/b exceeds 1.2 but others show maximum efficiencies for B/b=2.5 for narrow rotors ($4b/D_1=1.0$) [16].

The purpose of this paper is to investigate the relative influence of rotor and volute widths on fan characteristics, velocity profiles and losses in the volute. The experimental procedure includes standard fan characteristic measurements and then laser Doppler anemometry of the velocity profiles. Four rotors with different widths were tested inside two different volutes. The characteristic curves show the general effect of volute and rotor widths. Then a comparison between velocity profiles at selected points shows the ensuing changes in the flow field. The results are then discussed for a better knowledge of the flow and loss mechanisms inside the fan.

2 Experimental setup

The performance tests were according to BS-848, part 1, 1997 that is equivalent to ISO 5801-1997 [26]. A free inlet, ducted outlet configuration was selected for the experiments. A Pitot tube connected to an inclined manometer measured the total head at standard-defined locations inside the circular duct.

A two-component laser Doppler anemometer measured the velocity components at selected positions outside the rotors. It consisted of a 5 W Argon-ion laser that provided the 514.5 nm (green) and 488.0 nm (blue) beams. Necessary optics split each beam and a Bragg cell frequency shifted one beam from each pair by 40 MHz to remove directional ambiguity. A fiber optic system with beam spacing of 75 mm and focal length of 310 mm focused the beams on the desired measuring point and also collected the data in back scatter mode.

Beam refraction from side walls changed the movement of the measuring volume from that of the probe that resulted in errors in placing the measuring point. The calibration that corrected the difference was through first aligning the measuring volume with the front and back sidewalls of the fan. The probe movement was then divided to equal distances. Measuring volume dimensions were 0.100 x 0.097 x 0.417 mm^3 for green beams and 0.105 x 0.103 x 0.439 mm^3 for blue beams. Among the four fan configurations that were tested, the smallest rotor width was 123 mm and the largest volute width was 200 mms. Since the laser probe faced the fan from the back plate, the error in positioning the measuring volume changed between 0.2% of the traverse length (the volute width) and 0.35% of the rotor width.

The natural dust in the air provided adequate seeding such that data rates up to 0.8 kHz were maintained throughout the tests with over 80 percent validity. Two burst spectrum analyzers collected the data from the light fringes on two photomultipliers and the computer software processed the signals. Deviations from average velocity at the rotor outlet resulted in RMS values for the radial component at 100% or more. This unsteadiness was not just turbulence but jets and wakes out of the rotor that swept through the measuring volume. Turbulence is therefore superimposed over jets and wakes that were dominant ergodic unsteadiness and gave rise to bias error. The continuous data collection mode organized data collection at regular intervals and reduced bias error in velocity averaging (regardless of the selected averaging scheme) to less than 2% [27].

3 Fan performance

Four fans were constructed for the present experiments. They had four rotors with similar diameters and different widths. There were two volutes of different widths. The two narrower rotors were placed in the narrower volute and the two wider rotors in the wider volute. All other dimensions were the same. Fan dimensions are in Table 1. They are grouped into common fan parameters that are similar for all four fans and specific parameters to each fan. The ratio $4b/D_1$ changes from 1.73 to 2.32 for different rotors. The ratio of volute width to rotor width of these fans changes from 1.2 to 1.3. Machine Reynolds number was 3.4 x 10^5 for all experiments where the performance parameters were independent of Reynolds number [10].

The performance curves of the four fans are in figures 3a and b. Selected points (A to H) denoted on the curves were later used for Laser Doppler Anemometry. Before making any comments on these curves, figure 3c compares them with other available squirrel-cage fan performances in the literature. The curves for the present experiments are within the available range for such fans. Maximum fan flow rate is a function of volute spread angle. It was 5° for the present fans. An increase to a maximum of 11° would enhance flow rate to that of other performance curves with drawbacks for efficiency and head. Although all effort was made that optimum geometric values from other research should be used for the present fans, nevertheless, it is known that for any individual fan, added geometric optimization (inlet geometry for example) could further enhance fan performance [14].

Fan characteristics in figure 3a are in two different groups. First are the two in the narrow volute that decline faster with flow. The second group is the two characteristics from the fans

with the wider volute and in this case they show larger maximum flow rate and also a more flat characteristic. Such observations on width are new for squirrel cage fans and the first conclusion is a reconfirmation that volute dimensions could be one of the controlling parameters of the flow through the rotor and the fan. It was previously noted that a larger volute spread-angle allows a larger fan flow rate [10]. This figure shows that the wider volute allows more flow through the rotor in a similar way and also flattens the characteristic curve. A change of rotor width within the same volute, only marginally changes the maximum flow rate but the slope of the characteristic remains the same. Efficiency trends in figure 3b show that the two fans with the wider rotor ($4b/D_1$ = 2.11 and 2.32) and therefore a wider volute have efficiency peaks at larger flow coefficients. Points F and G (peaks of characteristics of fans with wider volute) are closely located on characteristic and efficiency curves. They are both more efficient than A and E (peaks of characteristics of fans with narrower volute) and therefore there is a more efficient momentum transfer for the wider volute regardless of the rotor size.

The common approach for squirrel-cage fan design is to find optimum rotor dimensions and then size the volute accordingly [10]. These results show that squirrel cage fan characteristics follow both the volute and the rotor dimensions. In a previous experiment, the flow coefficient was a function of volute spread angle and therefore it was proposed that a selection of spread angle first with a rotor that is accordingly sized would provide more optimum aerodynamics inside the fan [5]. A combination of these two results suggests that an alternative approach to fan design would be to size the fan based on volute parameters first and then select the rotor accordingly.

4 Procedure for laser Doppler anemometry

Characteristics of the four fans were discussed in the previous section. It is now accepted practice that there are corresponding behaviors between velocity fields and performance curves [8],[12] ,[14] and [28]. Laser Doppler anemometry is a point wise measuring technique and velocity fields change with operating point on the characteristics and peripheral, axial or radial location in each fan. Therefore regardless of its advantage of being non-intrusive, a comprehensive measurement of velocity profiles would be a rigorous task. Primary velocity measurements for limited but justified setups and positions, could show the trends in flow separation after the inlet and the non-uniform flow through the volute, and guide for more detailed experiments in the future.

a. The selection of the velocity test points A to H on the performance curves in figures 3a and b was based on two criteria:
    1- A comparison between points A, B, C and D on the characteristic of a fan with narrow volute and points G and H on the characteristic of a fan with wider volute could show the influence of flow rate and its dependence on width and velocity components.
    2- A comparison between points A, E, F, and G that have the maximum head coefficients of their respective characteristic could show the influence of fan width on velocity components at these points.
b. In order to select the angular positions on the volute for velocity measurements, it was reasoned that in a squirrel cage fan when the throttle is fully open, air flows out of the rotor at almost all circumferential locations (not uniform necessarily). When the fan is throttled, flow recirculation back into the rotor starts close to the cut-off. With further throttling, this recirculation occupies a larger portion of the rotor perimeter [16]. Two circumferential positions were therefore selected for velocity measurements:

1- The location at 270° (figure 1) which is away from the cut-off and could have outward flow everywhere on performance curves.
2- The location at 360° was also selected. Generally this position has outward flow from the rotor and could show flow reduction or even reversing flow back into the rotor due to its proximity to the cut-off.

No measurements was made at other circumferential positions since in squirrel cage fans with logarithmic spiral casing profiles, the small volute cross section at 90° and 180° passes a smaller portion of the flow out of the rotor even at fully open throttle [28].

c. Previous research on squirrel cage fan shows that there is a gentle radial velocity decay just after the rotor [14]. The intention for the present experiments was to measure the velocity profiles as close to the rotors as possible and at the same time far enough so that rotor back surface would not block any of the four laser beams; hence, the selected traverse radius for velocity measurements was at 1.17 times rotor diameters.

5 Interrelation between flow rate, fan width and velocity components

The purpose of this section is to show the inter-relation between fan characteristics and velocity components in selected positions with changes in rotor and volute widths. Selected performance points for velocity measurements are shown in figure 3. Velocity profiles at different operating conditions of fan 1, points A, B, C and D are in figures 4a and 4b. Velocity profiles of fan 4 at points G and H are in figures 5a and 5b. Although we use these profiles to judge the circumferential variations in through flow but this is not possible directly from the curves since each velocity profile has local variations that are ambiguous for overall judgments. Tables 2 to 4 clarify this point by providing non-dimensional integrals of the radial velocity profile (I) for each traverse of the laser probe across the width as calculated from equation 1.

$$I = \frac{\int_0^B v_r dz}{\pi D N b} \tag{1}$$

The first three lines of these tables are fan properties at specified points as extracted from characteristic tests. Lines 4 and 5 give the velocity integrals (I) for 270° and 360° and line 6 gives their sum. The last three lines are the flux of flow at the two measuring stations and their added contribution to the fan non-dimensional flow rate. Therefore characteristic curves (figure 3), velocity profiles (figures 4 to 6) and integrals of the velocity profiles (tables 2 to 4) are the instruments for the following discussion first on the flow field of a single fan and then on the effects of rotor and volute widths.

1. How does the relative size of the stall region behind the inlet change with flow rate in a fan with fixed geometry? Figures 4a and 4b show radial and tangential components of the velocity out of rotor for fan 1. Figure 4a (at 270°) has no indication of a change of the velocity profiles with flow. The small change in radial and tangential velocities in the stalled region behind the inlet ($0.7 < z/B < 1.0$) are indications of the re-circulating flow, and not the through flow [15]. On the contrary in figure 4b for 360°, the change in velocity profile due to flow rate is notable. The stalled region as judged from the radial profile after the inlet spans between $0.6 < z/B < 1.0$ for A (smaller flow rate) and reduces to $0.8 < z/B < 1.0$ for the larger flow rate at D (Inlet plane is at $z/B = 1.0$).
2. How does the flow distribution change round the rotor for a single fan with fixed geometry at different flow rates and how does the volute control this variation? The active part of the rotor is near the back plate where z direction originates (figures 1 and 2). As the flow rate increases in fan 1, the flow at 360° (figure 4b) is more sensitive to this

change than the flow at 270° (figure 4a). Table 2 confirms this where for an increase in the flow coefficient from 0.21 to 0.58 (176% increase), the defined integral (I) at 270° has only increased from 0.25 to 0.33 (32% increase) but the same integral at 360° has more than doubled from 0.29 to 0.63 (117% increase). It shows that for the narrower volute the added flow selects the widest cross section. Line 7 of table 2 shows that the share of 270° from the total flow almost halves (1.19 to 0.57; 52% reduction) while at 360°, the share of the total flow has had smaller change (1.38 to 1.086; 21% reduction) and the flow in this section changes almost proportional to the overall fan flow. Of course with this reduction of the share of these two sections to the total fan flow, the rest of the volute has taken a larger share of flow. This is confirmed in line 9 that shows when the flow rate increases (column A to column D), these two sections together take a smaller portion of the fan flow (2.57 to 1.655; 36% reduction).

Figure 5 plus table 3 show that for the wider volute (fan 4), with an overall increase in fan flow rate (ϕ_r = 0.37 to 0.55; 48.6% increase), the contribution of the section at 270° to the total flow between points G and H increases from 0.54 to 0.96 (78% increase). The share of the section at 360° has dropped from 0.946 to 0.52 (45% reduction). Line 9 shows the share of these two sections together from the overall fan flow has no considerable change (1.486 to 1.58; 6% increase) and therefore little change is expected in the proportional share of the flow at other sections round the volute.

The conclusion is that the distribution pattern of flow round the rotor for wider volute does not change considerably as the fan flow rate increases, but for the narrower volute the pattern would change and the added flow goes through the rotor at 360°. This conclusion complies with [28] that volute size controls the flow through the rotor and it is possible to change circumferential flow patterns with a different volute cross sectional area.

3. How does this peripheral flow distribution affect fan efficiency? This is an extension of the previous discussion that shows the two fans behave differently as the added flow due to a change in throttling could select an earlier or later circumferential location to exit the rotor. In fan 1 with the narrower volute the added flow rate, from condition A to condition D, goes through 360° and therefore from the rotor to the fan exit travels a shorter distance in the volute and thus efficiency increases with flow rate (figure 3b). Flow out of 270° would travel a longer distance in the volute as compared with 360° and therefore smaller efficiency was expected.

   Why the flow should exit the rotor at earlier or later circumferential locations for different geometric or flow conditions, is a subject for future investigations. One hypothesis is that if there is re-circulation back to the rotor close to cut-off, opening the throttle would activate larger parts of the rotor especially at cut-off and its vicinity. The second hypothesis is that since it is the volute size that controls the flow through the fan and the rotor, a larger cross-section inside the volute at any location brings about a smaller resistance there and this would enhance more flow through the rotor. The findings of this research seem to confirm the latter hypothesis. For fan 1 where volute width is smaller, the added flow selects to go through the rotor near the fan exit plane. In this fan the largest volute cross section is at 360°, and this has drawn added flow towards itself (table 2 and item 1 above). The ensuing increase in efficiency is due to the short path this flow turns inside the volute between the rotor and the exit plane. The wider volute of fan 4 has a larger cross section all around and therefore for a similar volumetric flow imposes less restriction at any circumferential location. Both of the above two hypotheses might be correct and each could take a share of the flow behavior in the figures.
4. A change in volute width or spread angle also changes the average velocity inside the volute for the same flow rate. Will a larger average velocity inside the volute reduce fan

efficiency? Flow coefficient ($\phi_r = 4Q/(\pi^2 ND^3)$) in figure 3 is non-dimensionalized with rotor peripheral velocity (πND) and inlet area (πD^2). There is no notion of rotor width in it and therefore it is termed radial flow coefficient. An alternative is to use rotor exit area (πDb) in the denominator. This would define the axial flow coefficient ($\phi_a = Q/(\pi^2 ND^2 b)$ that shows the volumetric flow rate per unit rotor diameter and rotor width and has the same value for two fans with different volute widths if their flow rates are also proportionately different. Such two fans have similar average velocities. With this in mind, it is now possible to compare the efficiency of point H with that of points C and D (figure 3). H and C have similar axial flow coefficients (ϕ_a). The efficiencies for H and C are close and therefore similar average velocities in the volute have resulted in comparable efficiencies. Next compare H and D that have similar radial flow coefficients (ϕ_r) but the axial flow coefficient is larger for D. This means that D has a similar volume flow as H but the volute cross section is smaller and therefore larger average velocities ensue. D is less efficient since at larger average velocities inside the volute, efficiency has dropped.

5. Points A and E (narrower volute) and F and G (wider volute) in figure 3 are peaks of the characteristics for each of the four fans. They are both the maximum heads and the left hand limit for the fan operating range. Figures 6a and 6b show the measured velocity components at sections 270° and 360° respectively. The corresponding integrals of the radial flow component across the width are in table 4. The velocity profiles are drawn with respect to non-dimensionalized volute width (z/B) and therefore any conclusions on changes of the stall size are independent of the respective volute size.
   Peaks of the characteristic curves for the narrower volute in figures 3a and 3b are at about half the flow rate of that of the wider volute. Table 4 shows, points F and G have 83% and 110% more flow than point E. At point G, the share of the fan total flow at 270° (0.54) has reduced to one third of that of E (1.61). The share of the flow at 360° has also reduced from 1.89 for a wider volute to 1.4 and then 0.94 (50% reduction) for the narrower volute. The total share of these two sections has reduced from 3.5 (wider volutes) to 1.97 and then 1.48 (narrower volutes) which is a 42% reduction. This repeats the observations of item 1 for different widths. A reduced throttling of the wider volute has activated larger portions of the fan periphery. Figure 6a shows that larger flow rate at 270° results in a smaller stall size (F and G; $0.4 < z/B < 1.0$ as compared to A and E; $0.6 < z/B < 1.0$, note also line 4 in table 4. No clear trend is evident at 360° (figure 6b) and therefore the conclusion is that wider volute has a smaller stall size even when it is throttled.

6 Conclusion

Performance characteristics and selected velocity measurements at the inlet to the volute of four squirrel cage fans show that volute width controls the flow round the rotor. A wider volute increases the maximum fan flow rate and makes fan characteristic more flat. Velocity profiles at the rotor exit show that flow distribution round the rotor is uneven. A wider volute and hence a larger cross section places less restriction on the flow and activates larger parts of the circumference.

Acknowledgement

The authors wish to thank Amirkabir University of technology for supporting this research.

References

[1] Eck, B., "Fans", 1st English Edition, Pergamon Press Oxford, pp. 117-140, (1973).

[2] Kim, K.W., and Seo, S.J., **"**Application of Numerical Optimization Technique to Design of Forward-Curved Blades Centrifugal Fan", JSME International Journal, Series B, Vol. 49, No 1. , (2006).

[3] Bayomi, N.N., Hafiz, A.A., and Osman, A.M., **"**Effect of Inlet Straighteners on Centrifugal Fan Performance", Energy Conversion and Management, Vol. 47, pp. 3307-3318, (2006).

[4] Kim, K.Y., and Seo, S.J., **"**Shape Optimization of Forward-Curved-Blade Centrifugal Fan with Navier-Stokes Analysis", Journal of Fluids Engineering, Vol. 126, pp. 735-742, (2004).

[5] Damangir, A., "Joint Impeller/Scroll Sizing of Squirrel Cage Fans using Alternative Non-dimensional Head and Flow Rate Coefficients", PhD thesis, Mechanical Engineering Department, Amirkabir University of Technology, (2004).

[6] Han, S.Y., and Maeng, J.S., **"**Shape Optimization of Cut-off in a Multi-Blade Fan/Scroll System using Neural Network", International Journal of Heat and Mass Transfer, Vol. 46, pp. 2833-2839, (2003).

[7] Toorani, A., **"**The Design of Squirrel Cage Fan Volute Profile with the Two Dimensional Uniform Flow Inverse Method", MSc thesis, Mechanical Engineering Department, Amirkabir University of Technology, (2000).

[8] Montazerin, N., Damangir, A., and Mirian, S., "A New Concept for Squirrel-Cage Fan Inlet", Journal of Power and Energy, Proceeding of Instn Mech Engrs, Vol. 212, pp. 343-349, (1998).

[9] Morinushi, K., "The Influence of Geometric Parameters on FC Centrifugal Fan Noise", Journal of Vibration, Acoustics, Stress, and Reliability in Design, Vol. 109, pp. 227-234, (1987).

[10] Roth, H.W.,"Optimierung Von Trommelläufer-Ventilatorn„ Strümungs Mechanik und Strümungs Maschinen, Vol. 29: pp. 1-45, (1981).

[11] Ballesteros, R., Velarde, S., and Santolaria, C., "Turbulence Intensity Measurements in a Forward-Curved Blades Centrifugal Fan". Proceedings of the XXIst IAHR Symposium on Hydraulic Machinery and Systems, Lausanne, September 9-12, (2002).

[12] Montazerin, N., Damangir, A., and Kazemi Fard, A., "A Study of Slip Factor and Velocity Components at the Rotor Exit of Forward-Curved Squirrel Cage Fans, using Laser Doppler Anemometry", Journal of Power and Energy, Proceeding of Instn Mech Engrs, Vol. 215, pp. 453-463, (2001).

[13] Velarde-Suarez, S., Ballasteros-Tajadura, R., Santolaria-Morros, C., and Gonzalez-Perez, J., "Unsteady Flow Pattern Characteristics Downstream of a Forward Curved

Blades Centrifugal Fans", Journal of Fluids Engineering, Vol. 123, pp. 265-270, June (2001).

[14] Montazerin, N., Damangir, A., and Mirzaei, H., "Inlet Induced Flow in Squirrel-Cage Fans", Journal of Power and Energy, Proceeding of Instn Mech Engrs, Vol. 214, pp. 243-253, (2000).

[15] Damangir, A., and Montazerin, N., "Stall Cells Inside the Volute of a Squirrel-Cage Fan", Proceeding of the Third Biennial Engineering System Design and Analysis Conference, Berlin, Germany, pp. 261-267, (1998).

[16] Ishihara, Y., and George, A.R., "Determination of Noise Sources in a Forward Curved Centrifugal Blower using Flow Visualization Methods", Proceeding of the noise-Con 94, Ft. Lauderdale, Florida, pp. 81-86. , (1994)

[17] Kind, R.J., and Tobin, M.J., "Flow in a Centrifugal Fan of the Squirrel Cage Type", ASME Journal of Turbo Machinery, Vol. 112, pp. 84-90, (1990).\

[18] Denger, G.R., and McBride, M.W., "Three-Dimensional Flow Field Characteristics Measured in a Forward-Curved Centrifugal Blower using Particle Tracing Velocimetry", Proceeding of Fluid Measurement and Instrumentation Forum, ASME Publication FED, Vol. 95, pp. 49-56, (1990).

[19] Raj, D., and Swim, W.B., "Measurement of Mean Flow Velocity and Velocity Fluctuations at the Exit of an FC Centrifugal Fan Rotor", ASME Journal of Engineering for Power, Vol. 103, pp. 393-399, (1981).

[20] Gessner, F.B., "An Experimental Study of Centrifugal Fan Inlet Flow and its Influence on Fan Performance", ASME paper, 67-FE-21, (1967).

[21] Ballesteros, R., Velarde, S., Hurtado, J.P., and Santolaria, C., **"**Numerical Calculation of Pressure Fluctuations in the Volute of a Centrifugal Fan", Journal of Fluids Engineering, Vol. 128, pp. 359-369, (2006).

[22] Lin, S.C., and Huang, C.L., **"**An Integrated Experimental and Numerical Study of Forward-Curved Centrifugal Fan", Experimental and Thermal Fluid Science, Vol. 26, pp. 421- 434, (2002).

[23] Japikse, D., Oliphant, K. N., and Pelton, R., **"**Optimization in Turbo Machinery Data Reduction", The 10th International Symposium on Transport Phenomena and Dynamics of Rotating Machinery, Honolulu, Hawaii, March 7-11, (2004).

[24] Brown, W.B., and Bradshaw, G.R., **"**Design and Performance of Family of Diffusing Scrolls with Mixed-flow Impeller and Vaneless Diffuser", NACA TR-936, pp. 305-314, (1947).

[25] Abidogun, K. B., and Ahmed, S.A., "Detailed Experimental Measurements of Flow Field Characteristics in a Radial Vane-less Diffuser", Proceedings of 2000 International Joint Power Generation Conference, Miami Beach, Florida, July 23-26, (2000).

[26] BS 848: Part 1, "Fans for General Purposes", Methods for Testing Performances, British Standard Institution, London, (1997).

[27] Johnson, D. A., Modarress, D., and Owen, F.K., "An Experimental Verification of Laser-Velocimeter Sampling Bias and its Correction", Trans ASME, J. Fluids Engng. Pwr, Vol. 106, pp. 5-12, (1984).

[28] Rezaie niya, S.M., Montazerin, N., Damangir, A., and Dehkordi, A.H., **"**Half Cone Rotors for Squirrel Cage Fans", Journal of Power and Energy, Proceeding of Instn Mech Engrs, Vol. 220, Part A:, pp. 753-763, (2006).

Nomenclature

b	rotor width
B	volute width
D_1	rotor inlet diameter
D_2	rotor outlet diameter
D_n	Inlet nozzle diameter
I	A non-dimensional number representing mass flow as defined in equation 1
N	rotational speed
P	pressure
r	radius
Re	machine Reynolds number = UD/ν
s	inlet spacing
U	rotor peripheral velocity
V_r	velocity; radial component
V_θ	velocity; tangential component
z	axial coordinate
Z	number of blades

Greek Symbols

α_s	volute spread angle
β_1	blade inlet angle
β_2	blade outlet angle
δ	Gap spacing
ϕ_a	Axial flow coefficient = $Q/(\pi^2 N D^2 b)$
ϕ_r	Radial flow coefficient = $4Q/(\pi^2 N D^3)$
γ	Cut off angle
θ	circumferential angle
ρ	Density
ψ	head coefficient = $2\Delta P/(\rho\pi^2 N^2 D^2)$
ν	kinematic viscosity

Tables

Table 1 Key dimensions for the fan.

common fan parameters			
D_1 (mm)	285	α_s (Deg)	5
D_2 (mm)	350	Z	43
β_1 (Deg)	90	N (rpm)	745
β_2 (Deg)	155	D_{inlet} (mm)	285

Specific parameters for each fan				
Fan	1	2	3	4
b (mm)	123	134	150	165
B (mm)	160	160	200	200
b/D_2	0.35	0.38	0.43	0.47
B/b	1.3	1.2	1.3	1.2
$4b/D_1$	1.726	1.881	2.105	2.316

Table 2 Integral of radial component of velocity profile (figure 4a and 4b) in the fan 1 on various points of performance curve

Line		Test point			
		A	B	C	D
1	ϕ	0.21	0.35	0.44	0.58
2	ψ	1.79	1.64	1.41	0.81
3	η	0.33	0.35	0.32	0.21
4	Integral (I) at 270°	0.25	0.3	0.27	0.33
5	Integral (I) at 360°	0.29	0.41	0.54	0.63
6	Sum of lines 4 and 5	0.54	0.71	0.81	0.96
7	$\frac{\text{Line 4}}{\text{Line 1}}$	1.19	0.85	0.61	0.57
8	$\frac{\text{Line 5}}{\text{Line 1}}$	1.38	1.17	1.22	1.086
9	$\frac{\text{Line 6}}{\text{Line 1}}$	2.57	2	1.84	1.655

Table 3 Integral of radial component of velocity profile (figure 5a and 5b) in the

fan 4 on various points of performance curve

Line		Test point	
		G	H
1	ϕ	0.37	0.55
2	ψ	1.89	1.71
3	η	0.39	0.30
4	Integral (I) at 270°	0.2	0.53
5	Integral (I) at 360°	0.35	0.29
6	Sum of lines 4 and 5	0.55	0.82
7	$\frac{\text{Line 4}}{\text{Line 1}}$	0.54	0.96
8	$\frac{\text{Line 5}}{\text{Line 1}}$	0.946	0.52
9	$\frac{\text{Line 6}}{\text{Line 1}}$	1.486	1.58

Table 4 Integral of radial component of velocity profile in the tested fans at maximum head

Line		Test point			
		E	A	F	G
1	ϕ	0.18	0.21	0.33	0.37
2	ψ	1.74	1.79	1.92	1.89
3	η	0.19	0.33	0.40	0.39
4	Integral (I) at 270°	0.29	0.25	0.19	0.2
5	Integral (I) at 360°	0.34	0.29	0.46	0.35
6	Sum of lines 4 and 5	0.63	0.54	0.65	0.55
7	$\frac{\text{Line 4}}{\text{Line 1}}$	1.61	1.19	0.57	0.54
8	$\frac{\text{Line 5}}{\text{Line 1}}$	1.89	1.38	1.4	0.94
9	$\frac{\text{Line 6}}{\text{Line 1}}$	3.5	2.57	1.97	1.48

Figures

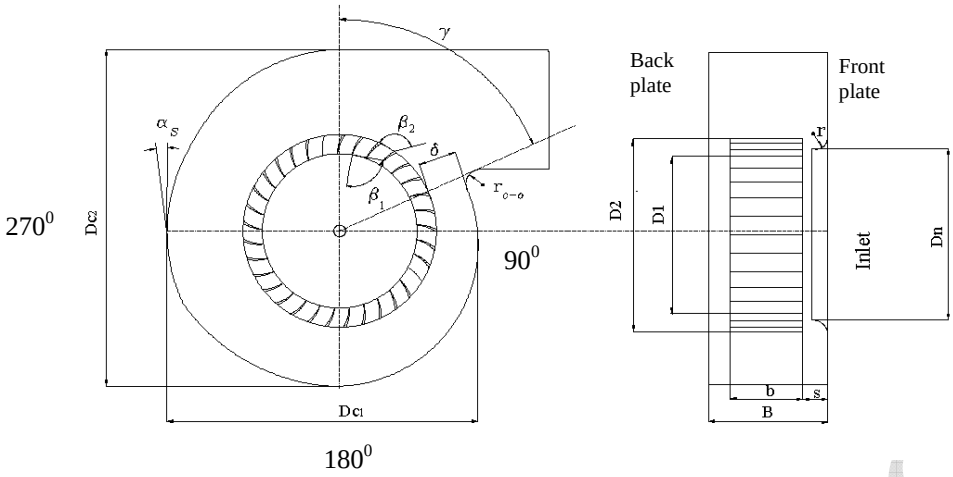

Figure 1 Schematic of squirrel cage fan

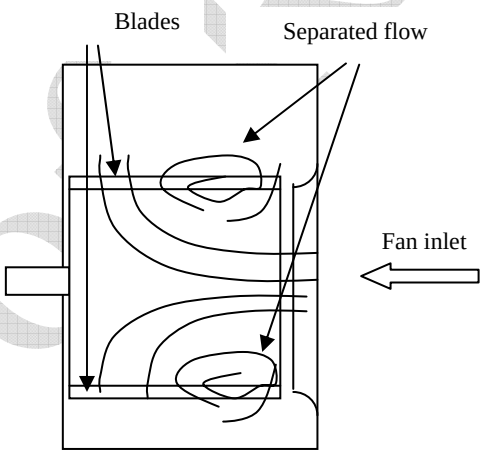

Figure 2 Schematic of flow field in the rotor of squirrel cage fans.

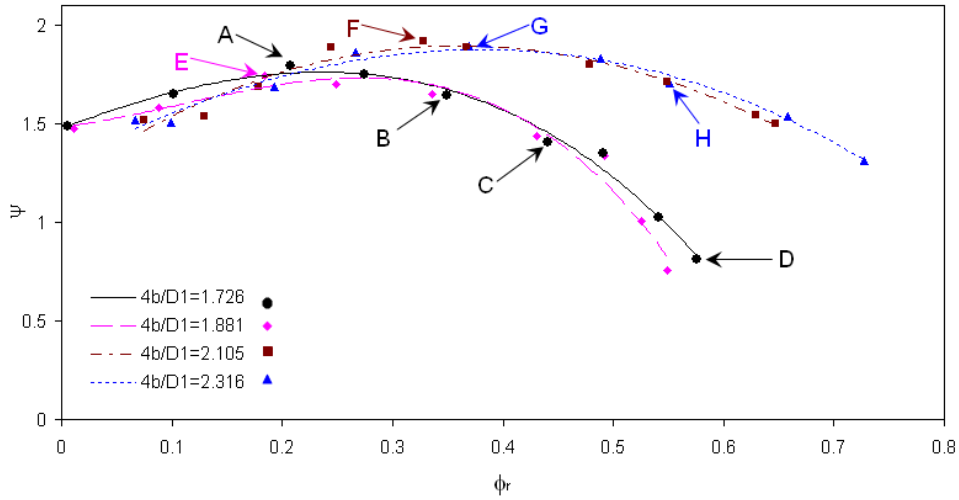

Figure 3a Fan performance based on radial flow coefficient

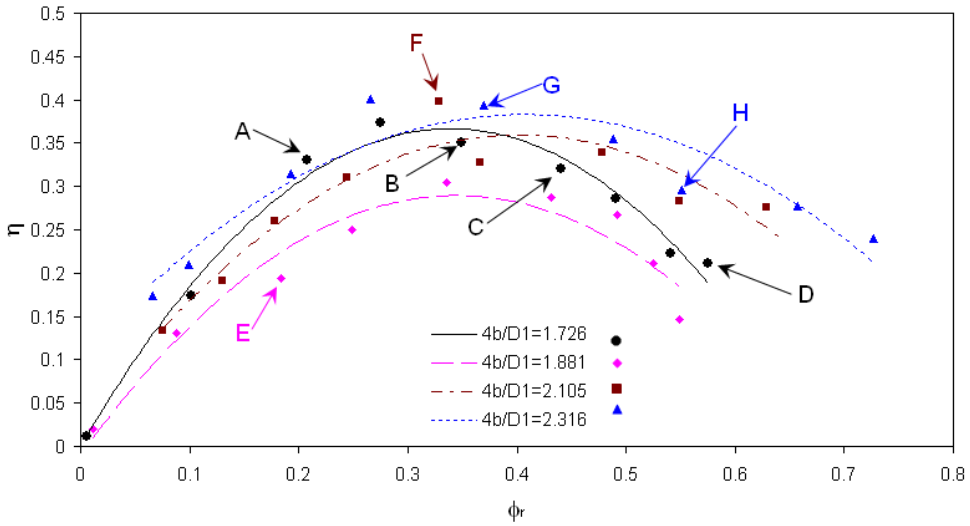

Figure 3b Fan efficiency curves

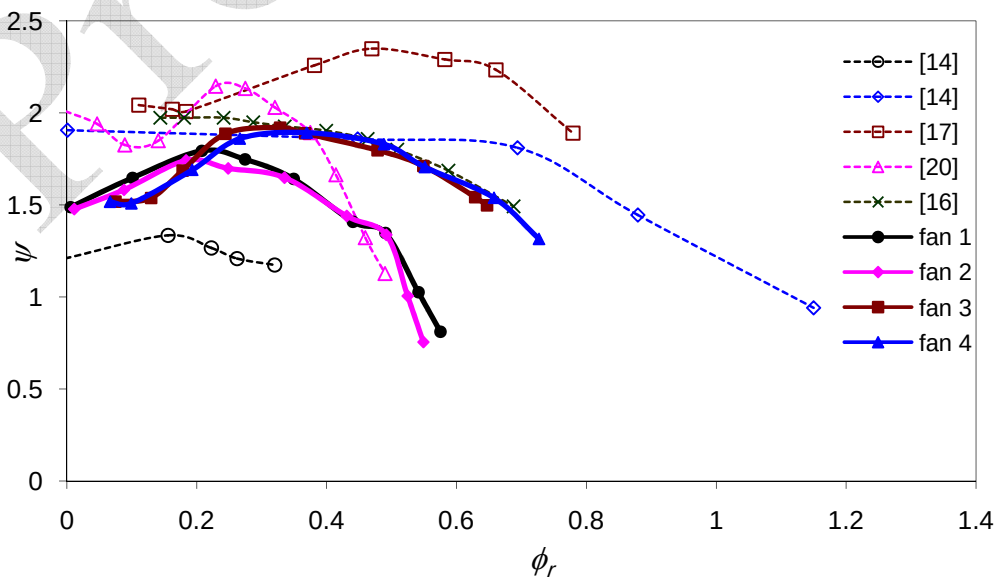

Figure 3c Comparison of performance curves with other available similar fan tests in the literature

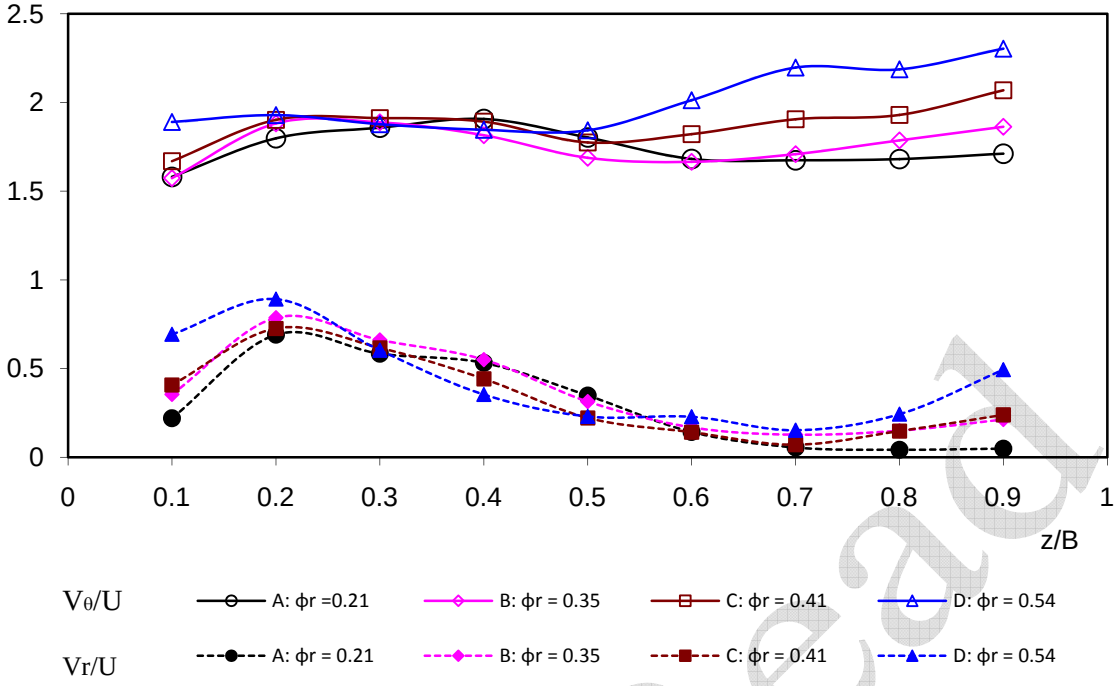

Figure 4a Radial and tangential components of velocity out of rotor, Fan 1, Section 270°

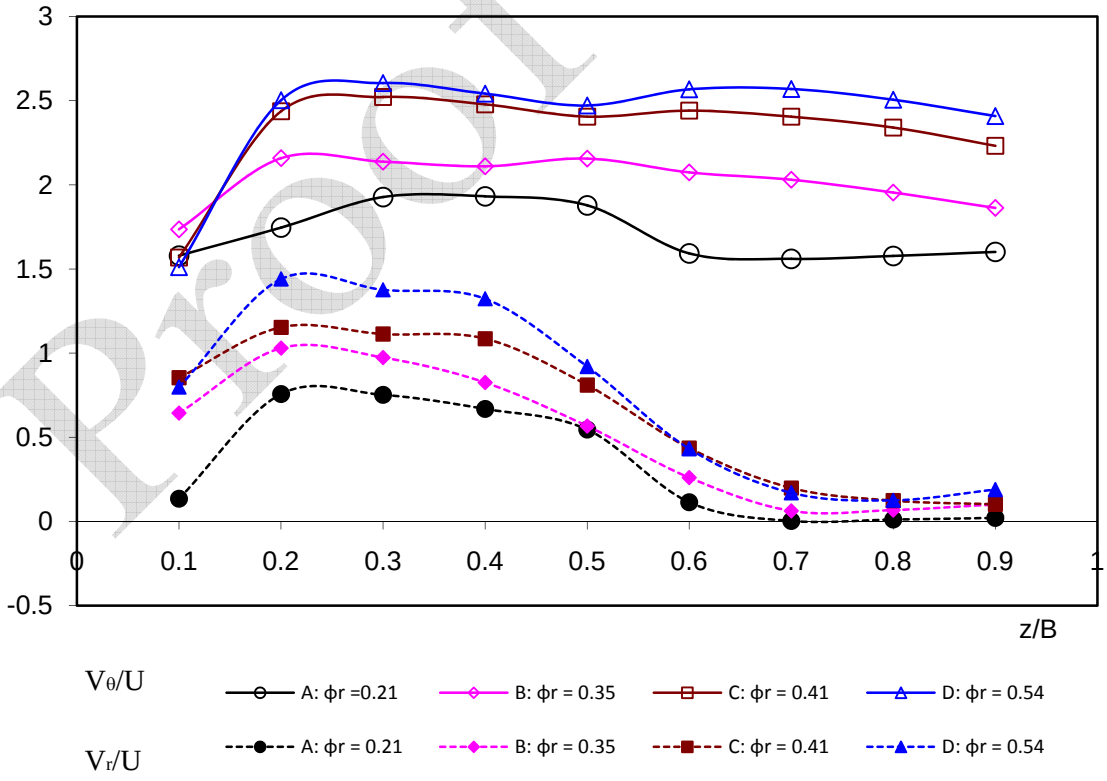

Figure 4b Radial and tangential components of velocity out of rotor, Fan 1, Section 360°

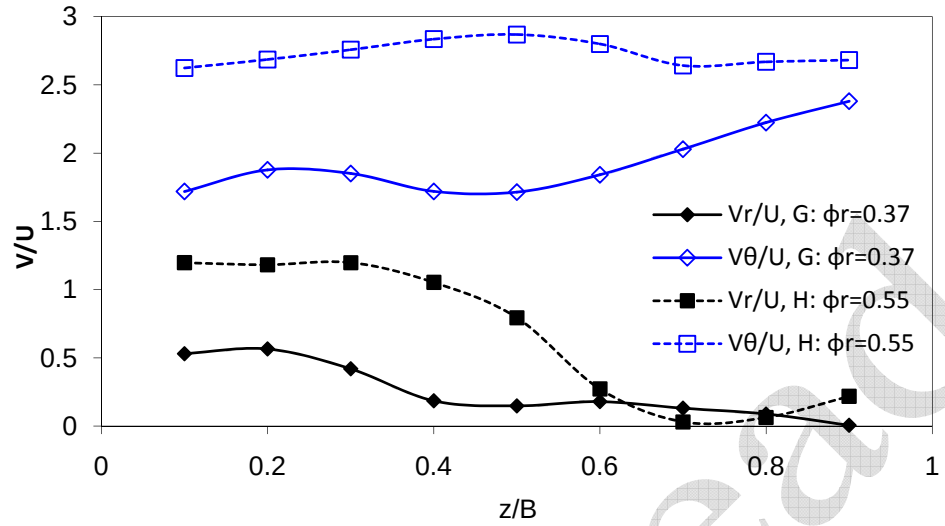

Figure 5a Radial and tangential components of velocity out of rotor, fan 4, section 270°

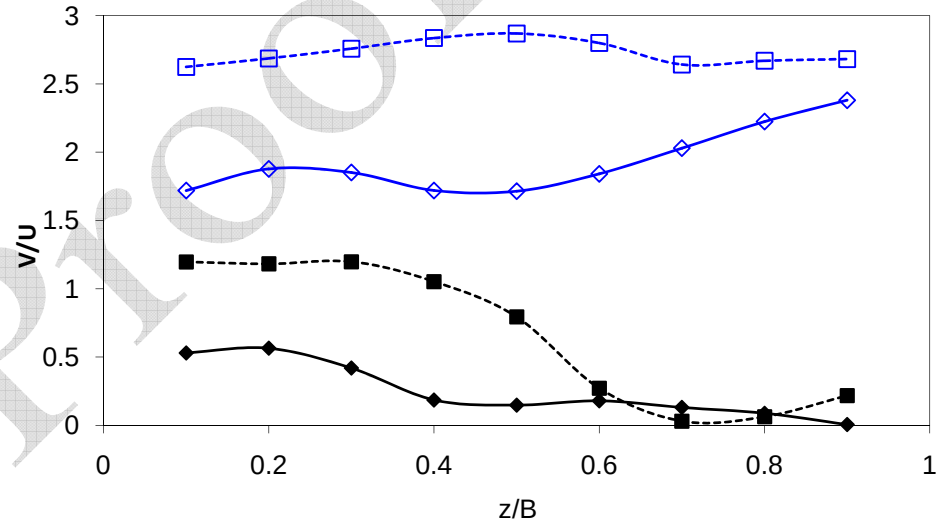

Figure 5b Radial and tangential components of velocity out of rotor, fan 4, section 360°

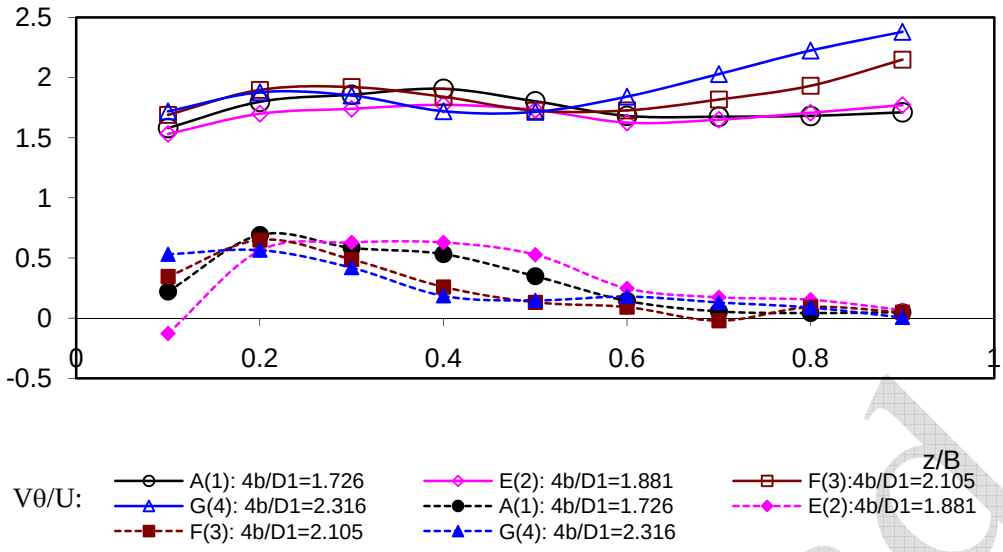

Figure 6a Radial and tangential components of velocity out of rotor, Section 270°
The legend refers to "point on the characteristic (fan number): rotor width"

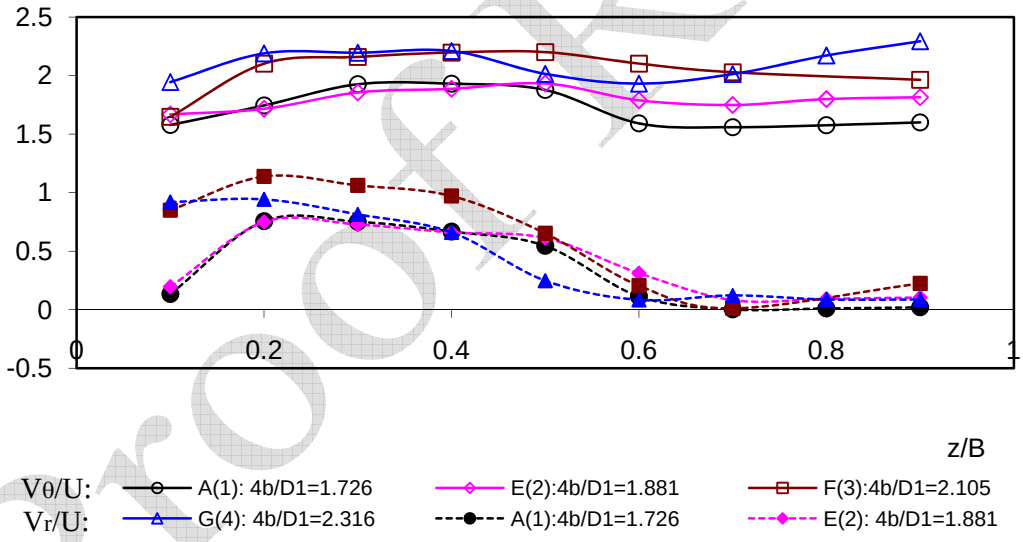

Figure 6b Radial and tangential components of velocity out of rotor, Section 360°
The legend refers to "point on the characteristic (fan number): rotor width"

چکیده

حلزونی فن لانه سنجابی با تنظیم جریان سیال درون روتور، تمامی فن را کنترل می نماید. آزمایش های عملکرد روی چهار روتور با قطر یکسان و عرض های متفاوت که درون دو حلزونی با عرض های متفاوت قرار داشتند نشان داد که عرض بیشتر حلزونی منحنی عملکرد را تخت تر کرده و حداکثر دبی عبوری درون فن را افزایش می دهد. اگر عرض حلزونی ثابت باشد، عرض روتور تنها حداکثر دبی فن را تغییر می دهد اما منحنی مشخصه تغییری نمی کند. پروفیل های سرعت بعد از روتور توسط لیزر داپلر اندازه گیری شدند. آنها نشان دادند که پروفیل های سرعت در زوایای مختلف حلزونی یکسان نیستند و شکل آنها برای عرض های مختلف حلزونی و شرایط مختلف عملکرد متفاوت می باشند. زمانی که مقاومت حلزونی بیشتر باشد، به دلیل سطح مقطع کوچک تر، بخش عمده جریان نزدیکتر به خروجی فن از روتور خارج می شود. این جریان تا رسیدن به خروجی فن، مسیر کوتاه تری درون حلزونی طی کرده و به همین دلیل راندمان فن بیشتر خواهد بود.